Photo-activation of persulfate and hydrogen peroxide by humic acid coated magnetic particles for Bisphenol A degradation

Nuno P.F Gonçalves, Marco Minella, Gilles Mailhot, Marcello Brigante, Alessandra Bianco Prevot

Catalysis Today xxx (xxxx) xxx–xxx

Contents lists available at ScienceDirect

Catalysis Today

journal homepage: www.elsevier.com/locate/cattod

Photo-activation of persulfate and hydrogen peroxide by humic acid coated magnetic particles for Bisphenol A degradation

Nuno P.F Gonçalves[a], Marco Minella[a,*], Gilles Mailhot[b], Marcello Brigante[b], Alessandra Bianco Prevot[a,*]

[a] Department of Chemistry, University of Turin, Torino, Italy
[b] Université Clermont Auvergne, CNRS, SIGMA Clermont, Institut de Chimie de Clermont-Ferrand, F-63000 Clermont-Ferrand, France

ARTICLE INFO

Keywords:
Heterogeneous Fenton
Magnetic particles
Humic acid
Hydrogen peroxide
Persulfate
AOPs

ABSTRACT

Magnetic particles (MPs) coated with humic acid (HA) prepared under anoxic atmosphere were tested as heterogeneous photo-Fenton catalyst for the activation of hydrogen peroxide (H_2O_2) and persulfate ($S_2O_8^{2-}$) using Bisphenol A (BPA) as a model pollutant. The role of HA coating, pH value and $H_2O_2/S_2O_8^{2-}$ concentration were investigated. A positive contribution of HA coating on H_2O_2 and $S_2O_8^{2-}$ activation was found. The highest BPA degradation rates were achieved at acidic conditions (pH 3) with both H_2O_2 and $S_2O_8^{2-}$, however persulfate showed a significant efficiency even at pH 6, interesting feature in the light of decreasing the wastewater treatment costs. By the addition of selective quenching agents, $^{\cdot}OH$ and $SO_4^{\cdot-}$ were identified as the main reactive species involved in the BPA abatement. An important contribution of the $S_2O_8^{2-}$ photolysis on the overall BPA transformation was highlighted. The reuse of the catalyst was investigated and similar efficiency using H_2O_2 and $S_2O_8^{2-}$ activation was observed until the third catalytic cycle. Experiments carried out using real wastewater samples, showed a good, even if less efficient compared to pure water, BPA removal.

1. Introduction

Among the advanced oxidation processes (AOPs), Fenton, photo-Fenton and Fenton-like processes have been attracting wide attention to degrade organic pollutants in water [1–3] due to their ability to generate highly reactive species able to abate biorecalcitrant species [4–6]. In the "classic" thermal Fenton process, the highly reactive species, mainly hydroxyl radical ($^{\cdot}OH$), but also superoxidized iron species [7] are generated by the reaction between Fe(II) ions and hydrogen peroxide. H_2O_2 forms an hydrated Fe(II)-H_2O_2 complex through the ligand exchange of a water molecule located in the first ligand sphere, then an inner-sphere two-electron-transfer gives an intermediate Fe(IV) complex which reacts with a molecule of water giving Fe^{3+} and $^{\cdot}OH$ [8].The reaction rate strongly depends on the pH with a maximum at pH 3, subsequently the treated solution has to be neutralized before its releasing, with sludge formation and increase of the overall cost of the process [9]. During the process the formation of hypervalent iron species (Fe^{4+}, as well as Fe^{5+} and Fe^{6+}) has been proven by stopped-flow experiments and UV/Vis spectroscopy [10]. The Fe^{3+} can be reduced to Fe^{2+} closing the cycle and making the process catalytic by H_2O_2 (with slow kinetics) or through an external energy input (e.g. photo-reduction of Fe^{3+} complexes in the so-called photo-Fenton process). A way to avoid the formation of useless and costly to be dismissed iron sludge at the end of the process is using iron-based catalyst easily to be recovered. In heterogeneous Fenton and photo-Fenton reactions the H_2O_2 is activated by iron supported in a solid matrix at acidic or even circumneutral pH. The catalyst recovery and the low amount of iron released in solution avoid the sludge formation and simplifies the process [11,12].

Similarly to the $^{\cdot}OH$, the sulfate radical ($SO_4^{\cdot-}$) has a high oxidation potential ($E_0(SO_4^{\cdot-}/SO_4^{2-}) = 2.43$ V vs NHE [13], being investigated for oxidation of recalcitrant pollutants [14–16]. The activation of persulfate and peroxymonosulfate ($S_2O_8^{2-}/SO_5^{2-}$) to generate $SO_4^{\cdot-}$ can be promoted by reactions of these precursors with iron both in the dark and under irradiation [17,18], in the presence and absence of ligands [19,20]. Additionally, the persulfate is described as less subject than $^{\cdot}OH$ to constituents of the real water samples, presenting an higher selectivity toward some pollutants [17,21]. Considering the usual low cost and quite high reactivity of the most common proposed iron-based catalysts, the activation of H_2O_2 and $S_2O_8^{2-}$ by these catalysts is raising growing interest in water treatment for emerging contaminant abatement [15,17]. The mechanism behind these

* Corresponding authors.
E-mail addresses: marco.minella@unito.it (M. Minella), alessandra.biancoprevot@unito.it (A. Bianco Prevot).

https://doi.org/10.1016/j.cattod.2019.12.028
Received 17 September 2019; Received in revised form 11 December 2019; Accepted 24 December 2019

heterogeneous processes has not been fully assessed yet, and it is worth to be studied in deeper details.

Fe_3O_4 magnetic particles (MPs) have been investigated as iron-source due to their Fenton catalytic activity, negligible toxicity, low-cost, facile recovery and recycling by means of a magnetic field [22]. Magnetite structure features a mixture of Fe(II)/Fe(III) oxide and it is well established the importance of Fe(II) ions for an active heterogeneous Fenton-like system [5,6,23]. Bare Fe_3O_4 MPs are susceptible to air oxidation and aggregation in aqueous systems. The stabilization with organic coating can reduce the oxidation of the magnetic phase (magnetite/maghemite) to hematite. Additionally, the introduction of humic(-like) substances, in both Fenton and photo-Fenton conditions appears to significantly enhance the pollutant degradation capacity [24,25], even though the effective role played by humic(-like) substances in the oxidation mechanism has not been already fully solved [26]. As an example, Aparicio and co-workers observed recently that core-shell magnetite-humic acids nanoparticles operate on the one hand as heterogeneous photosensitizers and on the other hand as catalysts in the photo-Fenton treatment for the oxidation of psychiatric drug carbamazepine. The MPs were excellent iron source promoting hydroxyl radical generation in the photo-Fenton process [27].

In this study, humic acid (HA) coated Fe_3O_4 magnetic particles (Fe_3O_4/HA) prepared by co-precipitation method under controlled conditions, were tested for H_2O_2 and $S_2O_8^{2-}$ activation under UVA/UVB irradiation in aqueous media using bisphenol A (BPA) as a model pollutant. Both processes, with H_2O_2 and $S_2O_8^{2-}$, are compared and the reactive species involved in the degradation were investigated through kinetic competition experiments using selective quenchers. The role of HA coating on the reactive species activation is also explored comparing the BPA abatement obtained with the hybrid catalyst with that observed with pristine MPs.

2. Materials and methods

2.1. Chemicals

H_2O_2 (30 % in water) was purchased from Fluka (France); BPA and $Na_2S_2O_8$ from Sigma (France); $FeCl_3{\cdot}6H_2O$ and $FeSO_4{\cdot}7H_2O$ from Carlo Erba Reagents (Italy); humic acid sodium salts (technical, 50–60 % as HA) from Aldrich-Chemie. Suspensions and standard solutions were prepared in Milli-Q water.

The Sewage Treatment Plant Water (STPW) was collected from the outflow (immediately before the last disinfection and the water discharge) of a wastewater treatment plant on NW of Italy (January 15th, 2019). Samples were used after a rough pre-filtration step, carried out through a grade qualitative filter paper (Whatman) removing large suspended solids and filtered using a hydrophilic 0.45 µm filter Sartolon Polyamide (Sartorius Biolab).

2.2. Preparation of MPs/HA

Humic coated magnetite particles were prepared by co-precipitation method under nitrogen atmosphere to avoid the Fe^{2+} oxidation, as previously reported [28]. Briefly, 35 mL of a solution of $FeCl_3{\cdot}6H_2O$ 0.68 M and $FeSO_4{\cdot}7H_2O$ 0.43 M (molar ratio Fe(III)/Fe(II) = 1.5) were added to 65 mL of deoxygenated water at 90 °C, under vigorous mechanic stirring and N_2 continuous flow. Then 10 mL of ammonium hydroxide (25 %) and 50 mL of 0.5 wt.% HA solution was added rapidly and sequentially. The mixture was dried for 30 min at 90 °C, and then kept to cool to r.t. under continuous nitrogen flow. The obtained MPs (Fe_3O_4/0.5HA) were centrifuged and washed with 40 mL water five times. The MPs were then dried in a Tube Furnace under nitrogen flow at 80 °C for 15 h and manually crumbled. The bare Fe_3O_4 MPs were prepared with the same procedure without the addition of HA solution. The selected loading of HA demonstrated the best reactivity both in the dark and under irradiation. For the in-depth characterization of these MPs refer to [28].

2.3. Methods

2.3.1. Degradation experiments under UVA/UVB irradiation

Irradiations were performed in a cylindrical Pyrex reactor, placed in a rectangular box equipped on the top with four lamps (Sankio denki G15T8E) emitting mainly in the UVA and UVB region. The emission spectrum was recorded using an optical fiber coupled with a CCD spectrophotometer (Ocean Optics USD 2000) calibrated with a Deuterium Tungsten Halogen reference lamp. A total irradiance between 265 and 400 nm of 2150 µW cm^{-2} was measured (see Fig. S1).

The experiments were performed at room temperature using a circulation cooling system. 50 mL of 100 mg/L MPs suspension and 20 µM BPA at adjusted pH with H_2SO_4 were sonicated for 20 min, then the H_2O_2 or $Na_2S_2O_8$ solutions were added. The suspension was magnetically stirred and placed under irradiation. At defined time interval 3 mL were sampled and the reaction immediately quenched with 200 µL of methanol. The samples were filtered using a 0.45 µm filter before the analysis.

The catalyst reusability experiments were performed by recovering the catalyst after 3 h under irradiation using a magnet. The recovered catalyst was 3 times washed and then dried at room temperature before being used in the next run.

The experiments with STPW were performed on BPA-spiked solutions. STPW samples had 14.25 mg_C L^{-1} of total organic carbon (TOC), 34.16 mg_C L^{-1} of inorganic carbon (IC), 7.74 mg_N L^{-1} of total nitrogen (TN) and pH value of 7.3.

2.3.2. Analysis

The concentration of BPA was measured through an ultra-performance liquid chromatography (UPLC) AQUITY (Waters, USA) equipped with photodiode array detector and by using a C18 AQUITY UPHLC BEH column (2.1 × 100 mm, 1.7 µm). The flow rate was 0.3 mL min^{-1} and the mobile phase was a mixture water methanol (60/40, v/v). The BPA concentration was quantified at 220 nm.

TOC, IC and TN were measured using a Shimadzu TOC-5000 analyzer (catalytic oxidation on Pt at 680 °C).

The determination of Fe released in solution was evaluated by a spectrophotometric procedure as reported in the Supplementary material (hereafter SM).

3. Results and discussion

3.1. H_2O_2 and $S_2O_8^{2-}$ activation

In order to evaluate the role of HA coating on the H_2O_2 and $S_2O_8^{2-}$ activation during the degradation of BPA, experiments were run by comparing the BPA degradation in the presence of both the hybrid MPs and the bare magnetite at different pH values. In all cases the BPA disappearance followed a pseudo-first order kinetics with an exponential decay ($C/C_0 = \exp(-k \times t)$, where C and C_0 are the BPA concentration at the irradiation time t and before irradiation, k is the pseudo-first order kinetic constant). Fig. 1a shows the BPA disappearance in the presence of H_2O_2. It was observed an enhancement of the activity promoted by the HA coating for all pH. In detail, at pH 3 the complete abatement of BPA was observed after 2 h in the presence of MPs/HA ($k = 0.034 \pm 0.003$ min^{-1}), while with the bare Fe_3O_4 only 80 % abatement was achieved ($k = 0.015 \pm 0.001$ min^{-1}), in agreement with results previously described [28]. A comparable tendency was observed in the presence of persulfate, as can be observed in Fig. 1b (e.g. $\frac{k_{pH=3}^{Fe_3O_4/0.5HA}}{k_{pH=3}^{Fe_3O_4}} = 2.344 \pm 0.096$). In the presence of H_2O_2 the BPA abatement was considerably slower for pH higher than 4, while the effect on the persulfate system was less significant. In fact, even at pH 6 after 2 h under irradiation, 80 % of BPA degradation was achieved

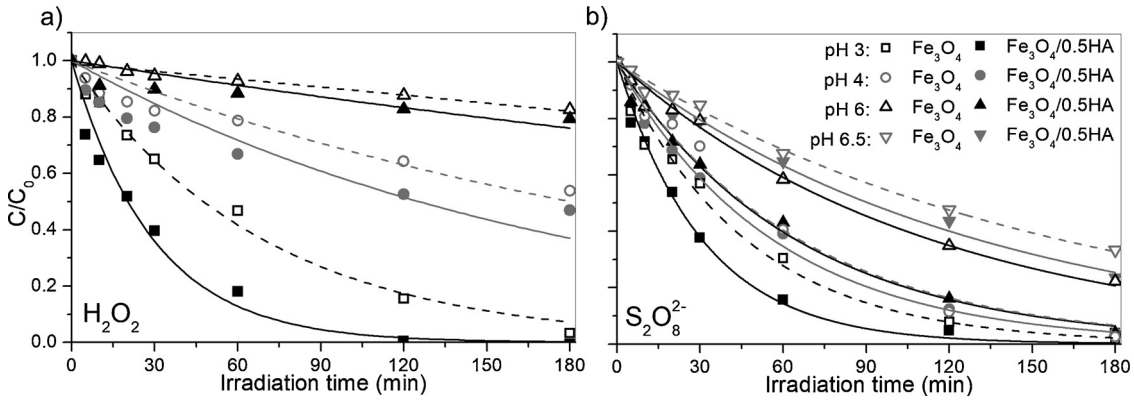

Fig. 1. BPA photo-degradation with 1 mM H_2O_2 (a), and 1 mM of $S_2O_8^{2-}$ (b) in the presence of bare Fe_3O_4 or Fe_3O_4/0.5HA (100 mg/L) at different pH. C_0^{BPA} = 20 μM.

using $S_2O_8^{2-}$ (despite ~15 % with H_2O_2). The initial rates recorded in all the experiments of Fig. 1 are reported in Table 1 of SM.

No significant BPA degradation was observed under direct photolysis or in the presence of Fe_3O_4/0.5HA under irradiation. On the contrary, both the photolysis of persulfate and H_2O_2 in the absence of the catalyst allowed a partial degradation of BPA, faster with $S_2O_8^{2-}$ than with H_2O_2 ($\frac{k^{S_2O_8^{2-}}}{k^{H_2O_2}}$ = 2.47 ± 0.08). This indicates that the investigated hybrid catalyst did not show any pure photocatalytic properties, while its activity was strictly related to its activation ability towards H_2O_2 and $S_2O_8^{2-}$, as shown in Fig. S2.

It is well established that the pH adjustment and its subsequent neutralization, before water discharge, is responsible for an important part of the cost on the Fenton-like processes [29]. Keep the system working at circumneutral pH can be determining for the process cost-effectiveness allowing the feasibility for its application as water treatment. Considering this and in the light of possible in real scenario applications, the further persulfate experiments were performed at pH 6 while in the case of hydrogen peroxide at pH 3 to keep the system active (at pH 6 the H_2O_2 activation by Fe_3O_4/0.5HA was negligible both in the dark and under irradiation, see Fig. 1a).

3.2. Contribution of homogeneous catalysis

It has been reported that the contribution of homogenous (photo)-Fenton promoted by Fe(II) and Fe(III) ions released in solution by magnetite-based materials can have a not negligible effect in the abatement of organic substrates [30]. In this work the influence of irradiation on the iron release (concentration and redox speciation) was evaluated by determining the concentration of iron in solution, keeping the solution in the dark or under irradiation at pH 3, 4 and 6. Fig. 2 shows the Fe(II) and Fe(III) concentration spectrophotometrically determined. At time zero (after the sonication period) it was observed a higher amount of Fe(II) with respect to Fe(III) in agreement with the absence of H_2O_2 - able to oxidize Fe(II) to Fe(III) - and the higher solubility of Fe(II) with respect to Fe(III) ($pKs_{Fe(OH)3}$ = 38.8, $pKs_{Fe(OH)2}$ = 15.1 [31]). In the dark it was not observed any increase of the released Fe(II) over time, while under irradiation the release of Fe (II) and Fe(III) (less marked, and only at pH 3) was more obvious. The photo-dissolution of the magnetite-based materials under irradiation has been largely reported as a consequence of the formation of surface complexes which may trap e_{CB}^- and (or) h_{VB}^+ efficiently, thus enhancing the photodissolution. Spinel type oxides (as the catalyst here tested), such as γ-Fe_2O_3 (maghemite) or Fe_3O_4, (magnetite) are known to be more easily photocorroded than hematite [32]. The solubility decrease of iron (hydr)oxides can explain the lower Fe(II) and Fe(III) ions concentration observed for the systems at higher pH in the absence of effective ligands for both Fe(II) and Fe(III).

The mechanism of the photodissolution of the catalyst is ultimately quite complex and the data here reported can only partially clarify it. The organic coating has an active role in the process especially because the carboxylic moieties at the surface are effective ligands for Fe^{+2} and Fe^{+3}. Moreover, these iron complexes at the surface are not only redox active species able to react with hydrogen peroxide or persulfate, but they are also photoactive species. Note that, the spectrophotometric method used to determine the iron concentration in solution was carried out on filtered solutions and consequently is silent on the concentration and speciation of the iron complexed by organic ligands at the surface of the catalyst.

The contribution of the iron released in solution on the initial BPA degradation was evaluated as follows: BPA and $H_2O_2/S_2O_8^{2-}$ were added to the supernatant solution after removing the heterogeneous catalyst by filtration. To evaluate the effect of the iron photo-dissolution, degradation experiments were performed with supernatant at time zero, but also with the solution after 2 h under irradiation. Fig. 3 shows

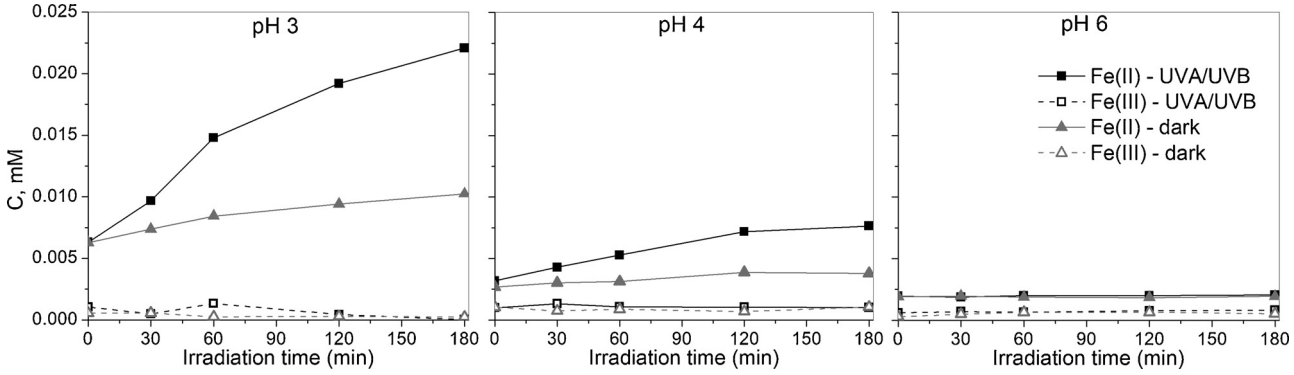

Fig. 2. Free Fe(II) and Fe(III) ions released in solution at pH 3, 4 and 6 by Fe_3O_4/0.5HA (100 mg/L) in the dark and under irradiation.

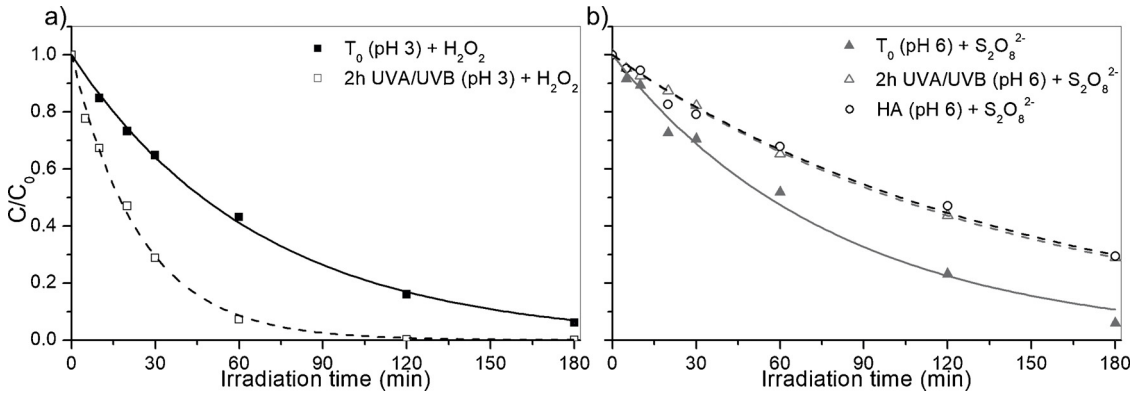

Fig. 3. BPA photodegradation in supernatant solutions obtained at time zero (T_0) and after 2 h of irradiation in the presence of 100 mg/L Fe_3O_4/0.5HA with H_2O_2 1 mM at pH 3(a) and $S_2O_8^{2-}$ 1 mM at pH 6 (b); BPA degradation with $S_2O_8^{2-}$ 1 mM and HA 0.4 mg/L).

the BPA degradation on supernatant at pH 3 after adding H_2O_2 (Fig. 3a) and on supernatant at pH 6 after $S_2O_8^{2-}$ addition (Fig. 3b). For both systems it was observed the BPA degradation in the homogenous phase. The addition of H_2O_2 to the pH 3 supernatant obtained after 2 h under irradiation allows to achieve a higher BPA degradation comparing with the corresponding supernatant at t_0. The higher concentration of iron resulted from the photo-dissolution of the catalyst. This tendency was not observed with persulfate. In fact, the supernatant at t_0 allowed to obtain higher BPA degradation than the supernatant after 2 h under irradiation. The low and stable over the time concentration of iron observed at pH 6 (Fig. 2), suggested an equal production of reactive species during the experiments with the two supernatants. The decreased rate of transformation observed with the supernatants obtained after 2 h of irradiation, can be explained considering the quenching effect of the HA that were partially released in solution from the organic coating, as previously reported with similar materials [33,34]. This was sustained by the negative effect observed on the BPA degradation when the direct photolysis of persulfate was carried out in solution containing HA (0.4 mg/L - the same HA amount added with 100 mg/L of catalyst – considering the HA loading equal 0.4 % w/w) which acted as efficient scavengers of reactive species (see Fig. 3).

3.3. Identification of reactive species

The reaction of H_2O_2 and $S_2O_8^{2-}$ with iron (in solution and/or at the catalyst surface, in the dark or under irradiation) can promote the formation of both $SO_4^{\cdot -}$ and $^{\cdot}OH$ according to the following reactions:

$$Fe^{2+} + S_2O_8^{2-} \rightarrow Fe^{3+} + SO_4^{2-} + SO_4^{\cdot}- \quad (1)$$

$$SO_4^{\cdot -} + OH^- \rightarrow SO_4^{2-} + {}^{\cdot}OH \text{ (relevant only under basic conditions)} \quad (2)$$

$$SO_4^{\cdot -} + H_2O \rightarrow HSO_4^- + {}^{\cdot}OH \quad (3)$$

$$Fe^{2+} + H_2O_2 \rightarrow Fe^{3+} + OH^- + {}^{\cdot}OH \quad (4)$$

$$Fe^{3+} + H_2O_2 \rightarrow Fe^{2+} + HO_2^{\cdot} + H^+ \quad (5)$$

$$Fe(OH)^{2+} + h\nu \rightarrow Fe^{2+} + {}^{\cdot}OH \quad (6)$$

Both $^{\cdot}OH$ and $SO_4^{\cdot -}$ can react not only with the contaminants, but also with the oxidants (Eqs. 7 and 9) which, at high concentration, are able to scavenge efficiently the reactive species depressing the overall reaction rate

$$SO_4^{\cdot -} + S_2O_8^{2-} \rightarrow S_2O_8^{\cdot -} + SO_4^{2-} \quad (7)$$

$$^{\cdot}OH + S_2O_8^{2-} \rightarrow S_2O_8^{\cdot -} + OH^- \quad (8)$$

$$^{\cdot}OH + H_2O_2 \rightarrow H_2O + HO_2^{\cdot} \quad (9)$$

Furthermore, under UVA/UVB irradiation the overlap between the emission spectrum of the adopted lamps and the absorption spectra of H_2O_2 and $S_2O_8^{2-}$ can promote the photolysis of both the oxidants [35].

$$S_2O_8^{2-} \xrightarrow{UVA/UVB} 2\,SO_4^{\cdot -} \quad (10)$$

$$H_2O_2 \xrightarrow{UVA/UVB} 2\,^{\cdot}OH \quad (11)$$

To understand the role of the generated reactive species involved in the investigated degradation processes, BPA photodegradation was carried out in the presence of radical scavengers (see Fig. S3). Isopropanol was used due to the high reactivity with hydroxyl radical ($k_{HO^{\cdot},\,isop} = 1.9 \times 10^9 M^{-1}s^{-1}$) [36]. With H_2O_2 we observed an almost complete inhibition of BPA degradation ($\frac{k^{H_2O_2}}{k^{H_2O_2}_{isop}} = 35.0 \pm 0.12$) indicating that the degradation is mainly due to the $^{\cdot}OH$ radicals.

The BPA degradation is strongly inhibited by isopropanol also in the case of $S_2O_8^{2-}$ ($\frac{k^{S_2O_8^{2-}}}{k^{S_2O_8^{2-}}_{isop}} = 11.06 \pm 0.09$). However, since isopropanol are able to quench both $^{\cdot}OH$ and $SO_4^{\cdot -}$ radicals ($k_{SO_4^{\cdot -},\,isop} = 8.6 \times 10^7 M^{-1}s^{-1}$) [37], the BPA degradation was carried out also in the presence of *t*-butanol that is a more selective quenching of $^{\cdot}OH$ ($k_{HO^{\cdot},\,t-but} = 3.1 \times 10^9 M^{-1}s^{-1}$), than of $SO_4^{\cdot -}$ ($k_{SO_4^{\cdot -},\,t-but} = 8.4 \times 10^5 M^{-1}s^{-1}$) [36,37]. Fig. S3 shows an only limited inhibition of the BPA degradation in the presence of *t*-butanol demonstrating that the degradation is mainly promoted by $SO_4^{\cdot -}$.

3.4. Effect of H_2O_2 and $S_2O_8^{2-}$ concentration

To elucidate the effect of H_2O_2 concentration on the catalytic system, experiments were performed by adding different H_2O_2 concentration (0.5, 1, 2, 3, 5 and 10 mM) at pH 3 (Fig. 5a) and pH 4 (Fig. 5b) in the presence of 100 mg/L of catalyst. The inset of Fig. 4a shows a quite complex behavior for the BPA initial transformation rate at pH 3, with an increment of the BPA degradation rate up to 1 mM, then a sharp decrease and for $[H_2O_2] > 3$ mM a further increase. While at pH 4 the highest degradation was achieved at 2 mM, but similar rates were observed for higher concentrations (see inset of Fig. 5a). This tendency can be only partially explained by the scavenging effect of H_2O_2 (Eq. 9) as often reported in the literature [38,39], because the decrease of the initial rate as a consequence of the increment of the oxidant concentration can justify a bell-profile and not a profile with a maximum and a minimum as that observed at pH 3. At high concentration of H_2O_2 a further process different to the photo-Fenton one (e.g. the direct photolysis of H_2O_2 which is a first order process with respect to hydrogen peroxide, and consequently increased linearly with the increase of the H_2O_2 concentration) might sustain the overall transformation compensating the scavenge of the $^{\cdot}OH$, formed through the reactions 4 and 7, by H_2O_2.

The BPA degradation was performed as well at different persulfate

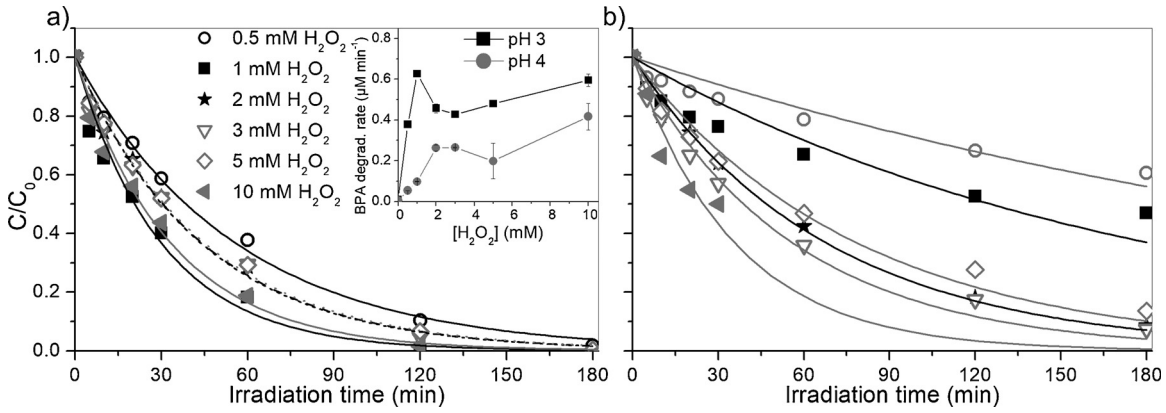

Fig. 4. Degradation profiles of BPA under irradiation with increasing concentration of initial H_2O_2 in the presence of Fe_3O_4/HA (100 mg/L) at pH 3 (a) and pH 4 (b). Inset of figure (a): initial BPA degradation rate as a function of the H_2O_2 concentration.

concentration (0.5, 1, 2, 3, 5 and 10 mM). Contrary of data obtained on H_2O_2 experiments, it was observed a monotonic increase of the rate rising the $S_2O_8^{2-}$ concentration (Fig. 5a). To split the contribution of the catalyst from that of the persulfate photolysis, the same experiments were carried out in the absence of the catalyst. The comparison among the rate is reported in Fig. 5b. We observed a different behavior at $[S_2O_8^{2-}]$ higher and lower than 2 mM. At $[S_2O_8^{2-}] < 2$ mM we recorded a positive effect of the presence of the iron-based catalyst, while at $[S_2O_8^{2-}] > 2$ mM the presence of Fe_3O_4/0.5HA had a negative effect, being the degradation rate higher without catalyst. This trend could be attributed to a scavenger effect from the HA acid coating, competing with the generated reactive species (see Section 3.2) and to the screening effect of the catalyst for the photons activating the photolysis of $S_2O_8^{2-}$ (the humic acid that can compete for the absorption of photons with the active iron-based species at the surface or in solution). In any case the behavior of the BPA transformation rate using different concentration of H_2O_2 and $S_2O_8^{2-}$ reported in Figs. 4 and 5 cannot be explained considering only the scavenging effect of H_2O_2 and $S_2O_8^{2-}$.

The recorded profiles are the results of a network of reactions composing the Fenton heterogeneous process (activated by H_2O_2 of $S_2O_8^{2-}$) which complexity has been already evidenced in some previously published articles [40–44]; for instance among the experimental parameters also the wavelength range of the irradiation showed to play a not negligible role.

Note that too high concentrations of $S_2O_8^{2-}$ must be avoided because the higher is the concentration of persulfate, the higher is the concentration of sulfate (the last product of the persulfate activated processes) in the final treated water. As an example, the Italian legislation imposed for the discharge of water in surface bodies a concentration of $SO_4^{2-} < 1000$ mg/L (10.4 mM) [45]. This value might be easily exceeded by treating the wastewater with persulfate at concentration higher than 5 mM (in this case the water should be furtherly treated after the heterogeneous photo-Fenton process to remove the excess of sulfate before the discharge). Carrying out the photo-Fenton process with H_2O_2 the same problem might be met. It is true that if H_2O_2 reacts completely the final products are environmental benign, but the need to carry out the photo-Fenton process at pH 3 and the successive phase of neutralization give very salted water that must be further treated before the discharge.

3.5. Catalyst recover and reuse

The catalyst reusability was tested by magnetically recovering the catalyst at the end of the BPA degradation. The catalyst was washed with water and dried before use for the next run. Fig. S4 shows the BPA abatement in 3 consecutive runs in the presence of H_2O_2 at pH 3 and $S_2O_8^{2-}$ at pH 6. At pH 6 in the presence of $S_2O_8^{2-}$ no decrease of activity was observed, while at pH 3 in the presence of H_2O_2 a very slight decrease on BPA abatement was observed. In both cases the tested catalyst did not show a significant deactivation/poisoning with the use.

3.6. Effect of water matrix composition

The influence of water matrix composition on H_2O_2- and $S_2O_8^{2-}$-based process was evaluated by comparing BPA degradation in STPW samples and in ultrapure water. Fig. S5 shows the BPA degradation profiles, a different behavior with H_2O_2 (pH 3) and $S_2O_8^{2-}$ (pH 6) was observed. With H_2O_2 the BPA degradation profile did not follow a first-

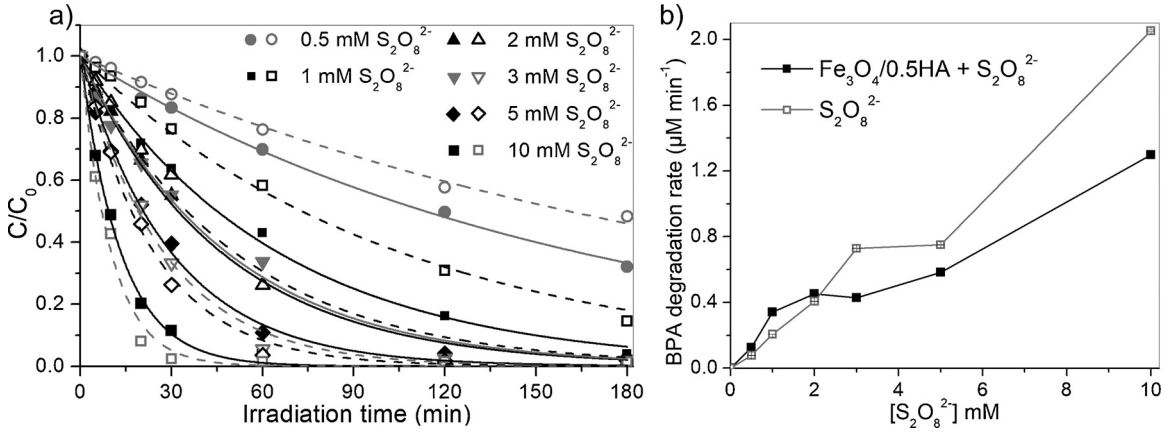

Fig. 5. a) BPA degradation profiles in the presence (full symbols) and absence (empty symbols) of Fe_3O_4/0.5HA (100 mg/L) at pH 6 using different $S_2O_8^{2-}$ concentrations. b) BPA initial degradation rate with and without Fe_3O_4/0.5HA particles in the presence of different $S_2O_8^{2-}$ concentrations.

order kinetics. The initial rate in real matrix was higher than in ultrapure water, but after 30 min the process slowed down giving after 3 h a lower degradation than in ultrapure water. A hypothesis is that the presence of organic species able to act as iron ligands gave an initial higher concentration of iron in solution able to react with H_2O_2, then the higher concentration of organic/inorganic scavengers partially block the reaction. With persulfate, the BPA degradation followed in both cases a pseudo-first order kinetics, but due to the high concentration of organic and inorganic scavengers [46,47] in the STPW the rate was roughly 4 times lower ($\frac{k^{S_2O_8^{2-}}_{Milli-Q}}{k^{S_2O_8^{2-}}_{STPW}} = 4.43 \pm 0.10$). The STPW sample used to simulate a real-word scenario had 2.7 $mg_C\ L^{-1}$ dissolved organic carbon, 41.1 $mg_C\ L^{-1}$ dissolved inorganic carbon, pH = 7.6 and 0.14 μS cm^{-1} conductivity. It is quite difficult on the basis of the composition of the water only, give more insights into the role that the specific components of the matrix have on modifying the rate of BPA transformation. Nevertheless, it is possible to hypothesize that the presence of hydroxyl and sulfate radical scavengers can limit the overall degradation. For instance, it is well know that organic matter is an important radical scavenger [35]. Moreover, the presence of inorganic carbon can lead to the formation of carbonate radicals ($CO_3^{\cdot -}$), less reactive towards BPA than $^{\cdot}OH$ and $SO_4^{\cdot -}$ as previously reported ($k_{HO^{\cdot},BPA} = 8.6 \times 10^9 M^{-1}s^{-1}$; $k_{SO_4^{\cdot -},BPA} = 4.7 \times 10^9 M^{-1}s^{-1}$; $k_{CO_3^{\cdot -},BPA} = 9.2 \times 10^7 M^{-1}s^{-1}$) [35].

4. Conclusions

Coating F_3O_4 with HA efficiently induced higher H_2O_2 and persulfate activation for the BPA removal at different pH, comparing with the pristine magnetite. The Fe_3O_4/0.5HA showed high capability to activate H_2O_2 at pH 3 with a substantial decrease of activity at pH higher than 4, while in the presence of persulfate even at pH 6 the system was still able to efficiently remove BPA. Both with H_2O_2 and $S_2O_8^{2-}$, the heterogeneous photo-Fenton process here investigated was operational in real wastewater, even if with lower kinetics than in ultrapure water.

The main reactive species involved in the process catalyzed by Fe_3O_4/0.5HA were $^{\cdot}OH$ (in the presence of H_2O_2) and $SO_4^{\cdot -}$ (in the presence of $S_2O_8^{2-}$).

The recovery experiments highlighted no significant loss of activity with the reuse of the material both with H_2O_2 at pH 3 and $S_2O_8^{2-}$ at pH 6.

With H_2O_2 (at pH 3) the photo-Fenton process in the presence of Fe_3O_4/0.5HA gave always better results than the "pure" photolysis of hydrogen peroxide, while with $S_2O_8^{2-}$ the presence of the catalyst gave a positive effect in comparison with the persulfate photolysis at $[S_2O_8^{2-}] < 2$ mM (note that $[S_2O_8^{2-}] > 5$ mM have to be avoided to prevent the production of final water with a sulfate concentration exceeding the law limits). At the same time, the photo-Fenton process at pH 3 can give after the final neutralization very salted water that must be further treated before the discharge.

CRediT authorship contribution statement

Nuno P.F Gonçalves: Investigation, Writing - original draft. **Marco Minella:** Conceptualization, Writing - review & editing, Supervision. **Gilles Mailhot:** Writing - review & editing. **Marcello Brigante:** Supervision, Writing - review & editing. **Alessandra Bianco Prevot:** Conceptualization, Writing - review & editing, Funding acquisition.

Declaration of Competing Interest

The authors declare that they have no known competing financial interests or personal relationships that could have appeared to influence the work reported in this paper.

Acknowledgements

This work is part of a project that has received funding from the European Union's Horizon 2020 research and innovation programme under the Marie Skłodowska-Curie grant agreement No 765860. Authors also acknowledge the financial support for experiments provided by the Region Council of Auvergne, from the "Féderation des Recherches en Environnement" through the CPER "Environment" founded by the Region Auvergne, the French government, FEDER from the European Community and from CAP 20e25 I-site project.

Appendix A. Supplementary data

Supplementary material related to this article can be found, in the online version, at doi:https://doi.org/10.1016/j.cattod.2019.12.028.

References

[1] S.D. Richardson, T.A. Ternes, Anal. Chem. 90 (2018) 398–428.
[2] M. Salimi, A. Esrafili, M. Gholami, A. Jonidi Jafari, R. Rezaei Kalantary, M. Farzadkia, M. Kermani, H.R. Sobhi, Environ. Monit. Assess. 189 (2017) 414–436.
[3] C. Byrne, G. Subramanian, S.C. Pillai, J. Environ. Chem. Eng. 6 (2018) 3531–3555.
[4] A. Mirzaei, Z. Chen, F. Haghighat, L. Yerushalmi, Chemosphere 174 (2017) 665–688.
[5] A.D. Bokare, W. Choi, J. Hazard. Mater. 275 (2014) 121–135.
[6] S. Enami, Y. Sakamoto, A.J. Colussi, Proc. Natl. Acad. Sci. 111 (2014) 623–628.
[7] C. Minero, M. Lucchiari, V. Maurino, D. Vione, RSC Adv. 3 (2013) 26443–26450.
[8] S.H. Bossmann, E. Oliveros, S. Göb, S. Siegwart, E.P. Dahlen, L. Payawan, M. Straub, M. Wörner, A.M. Braun, J. Phys. Chem. A 102 (2002) 5542–5550.
[9] M. Minella, S. Giannakis, A. Mazzavillani, V. Maurino, C. Minero, D. Vione, Chemosphere 186 (2017) 185–192.
[10] D.A. Wink, R.W. Nims, J.E. Saavedra, W.E. Utermahlen, P.C. Fords, Proc. Natl. Acad. Sci. 91 (1994) 6604–6608.
[11] M. Usman, J.M. Byrne, A. Chaudhary, S. Orsetti, K. Hanna, C. Ruby, A. Kappler, S.B. Haderlein, Chem. Rev. 118 (2018) 3251–3304.
[12] M.I. Litter, M. Slodowicz, J. Adv. Oxid. Technol. 20 (2016).
[13] R.E. Huie, C.L. Clifton, P. Neta, Radiat. Phys. Chem. (1991) 477–481.
[14] S. Wacławek, H.V. Lutze, K. Grübel, V.V.T. Padil, M. Černík, D.D. Dionysiou, Chem. Eng. J. 330 (2017) 44–62.
[15] I.A. Ike, K.G. Linden, J.D. Orbell, M. Duke, Chem. Eng. J. 338 (2018) 651–669.
[16] L.W. Matzek, K.E. Carter, Chemosphere 151 (2016) 178–188.
[17] P. Avetta, A. Pensato, M. Minella, M. Malandrino, V. Maurino, C. Minero, K. Hanna, D. Vione, Environ. Sci. Technol. 49 (2015) 1043–1050.
[18] A. Jonidi Jafari, B. Kakavandi, N. Jaafarzadeh, R. Rezaei Kalantary, M. Ahmadi, A. Akbar Babaei, J. Ind. Eng. Chem. 45 (2017) 323–333.
[19] Y. Wu, A. Bianco, M. Brigante, W. Dong, P. de Sainte-claire, K. Hanna, G. Mailhot, Environ. Sci. Technol. 49 (2015) 14343–14349.
[20] X. Wang, W. Dong, M. Brigante, G. Mailhot, Appl. Catal. B Environ. 245 (2018) 271–278.
[21] Y. Yuan, F. Geng, B. Shi, B. Lai, Environ. Eng. Sci. 36 (2018) 12–22.
[22] F. Franzoso, R. Nisticò, F. Cesano, I. Corazzari, F. Turci, D. Scarano, A. Bianco Prevot, G. Magnacca, L. Carlos, D.O. Mártire, Chem. Eng. J. 310 (2017) 307–316.
[23] J. He, X. Yang, B. Men, D. Wang, J. Environ. Sci. 39 (2016) 97–109.
[24] X. Ou, X. Quan, S. Chen, H. Zhao, Y. Zhang, J. Agric. Food Chem. 55 (2007) 8650–8656.
[25] S. García-Ballesteros, J. Grimalt, S. Berto, M. Minella, E. Laurenti, R. Vicente, M.F. López-Pérez, A.M. Amat, A. Bianco Prevot, A. Arques, ACS Omega 3 (2018) 13073–13080.
[26] L. Carlos, D.O. Mártire, M.C. Gonzalez, J. Gomis, A. Bernabeu, A.M. Amat, A. Arques, Water Res. 46 (2012) 4732–4740.
[27] F. Aparicio, J.P. Escalada, E. De Gerónimo, V.C. Aparicio, F.S.G. Einschlag, G. Magnacca, L. Carlos, D.O. Mártire, Nanomaterials 9 (2019) 1–12.
[28] N.P.F. Gonçalves, M. Minella, D. Fabbri, P. Calza, C. Malitesta, E. Mazzotta, A. Bianco Prevot, Chem. Eng. J. (2019) submitted.
[29] M. Minella, N. De Bellis, A. Gallo, M. Giagnorio, C. Minero, S. Bertinetti, R. Sethi, A. Tiraferri, D. Vione, ACS Omega 3 (2018) 9407–9418.
[30] M. Minella, G. Marchetti, E. De Laurentiis, M. Malandrino, V. Maurino, C. Minero, D. Vione, K. Hanna, Appl. Catal. B Environ. 154–155 (2014) 102–109.
[31] D.C. Harris, W.H. Freeman (Ed.), Quantitative Chemical Analysis, 2010 (USA).
[32] M.I. Litter, M.A. Blesa, Can. J. Chem. 70 (1992) 2502–2510.
[33] J. Liu, Z. Zhao, G. Jiang, Environ. Sci. Technol. 42 (2008) 6949–6954.
[34] J. Gomis, M.G. Gonçalves, R.F. Vercher, C. Sabater, M.-A. Castillo, A. Bianco Prevot, A.M. Amat, A. Arques, Catal. Today 252 (2015) 177–183.
[35] W. Huang, A. Bianco, M. Brigante, G. Mailhot, J. Hazard. Mater. 347 (2018) 279–287.
[36] G.V. Buxton, C.L. Greenstock, W.P. Helman, A.B. Ross, J. Phys. Chem. Ref. Data 17 (1988) 513–886.
[37] C.L. Clifton, R.E. Huie, Int. J. Chem. Kinet. 21 (1989) 677–687.
[38] J. De Laat, H. Gallard, Environ. Sci. Technol. 33 (1999) 2726–2732.

[39] H. Gallard, J. De Laat, Water Res. 34 (2000) 3107–3116.
[40] H. Kusic, I. Peternel, S. Ukic, N. Koprivanac, T. Bolanca, S. Papic, A.L. Bozic, Chem. Eng. J. 172 (2011) 109–121.
[41] M. Khandarkhaeva, A. Batoeva, M. Sizykh, D. Aseev, N. Garkusheva, J. Environ. Manage. 249 (2019) 109348.
[42] M. hui Zhang, H. Dong, L. Zhao, D. xi Wang, D. Meng, Sci. Total Environ. 670 (2019) 110–121.
[43] D. Zhao, X. Liao, X. Yan, S.G. Huling, T. Chai, H. Tao, J. Hazard. Mater. 254–255 (2013) 228–235.
[44] J.J. Pignatello, E. Oliveros, A. MacKay, Crit. Rev. Environ. Sci. Technol. 36 (2006) 1–84.
[45] D. Lgs 3 April. 2006, n. 152, https//www.gazzettaufficiale.it/atto/stampa/serie_generale/originario.
[46] E. Ortega-Gómez, M.M.B. Martín, B.E. García, J.A. Sánches Pérez, P. Fernández Ibáñez, Appl. Catal. B Environ. 149 (2014) 484–489.
[47] N. Rioja, S. Zorita, F.J. Peñas, Appl. Catal. B Environ. 180 (2016) 330–335.